Large isotopic shift in volcanic plume CO2 prior to a basaltic paroxysmal explosion

Fiona D D'Arcy[1], Alessandro Aiuppa[2], Fausto Grassa[3], Andrea Luca Rizzo[4], and John Stix[1]

[1]McGill University
[2]Università di Palermo
[3]Istituto Nazionale di Geofisica e Vulcanologia
[4]University of Milano-Bicocca

December 10, 2023

Abstract

Carbon dioxide is a key gas to monitor at volcanoes because its fluctuation relative to other gases can be detected prior to eruptions, yet carbon isotopic fluctuations at volcanic summits are not well constrained. Here, we present carbon isotopes measured from plume samples collected at Stromboli volcano, Italy, by Unoccupied Aerial System (UAS). We found contrasting volcanic source δ13C in 2018 during quiescence (-0.36 ± 0.59 paroxysm (-5.01 +- 0.56 of CO2-rich magma began degassing at deep levels (~100 MPa) in an open system fashion, causing strong isotopic fractionation and maintaining high CO2/St ratios in the gas. This influx occurred between 10 days prior to the event and up to several months beforehand, meaning that isotopic changes in the gas could be detected weeks to months before unrest.

Hosted file

980305_0_art_file_11620524_s4kdjv.docx available at https://authorea.com/users/704721/articles/690151-large-isotopic-shift-in-volcanic-plume-co2-prior-to-a-basaltic-paroxysmal-explosion

Large isotopic shift in volcanic plume CO_2 prior to a basaltic paroxysmal explosion

Fiona D'Arcy[1], Alessandro Aiuppa[2], Fausto Grassa[3], Andrea Luca Rizzo[4,5], John Stix[1]

[1] Department of Earth & Planetary Sciences, McGill University, Montreal, Canada
[2] Dipartimento DiSTeM, Università degli Studi di Palermo, Palermo, Italy
[3] Istitutio Nazionale di Geofisica e Vulcanologia, Palermo, Palermo, Italy
[4] Department of Earth and Environmental Sciences, University of Milano-Bicocca, Piazza della Scienza 4, 20126, Milan, Italy
[5] Istitutio Nazionale di Geofisica e Vulcanologia, Sezione di Milano, Via Alfonso Corti 12, Milan, Italy

Corresponding author: Fiona D'Arcy (fiona.darcy@mail.mcgill.ca)

Key Points:

- Rapid collection of volcanic plume CO_2 enabled by Unoccupied Aerial Systems
- A carbon isotopic anomaly was present 2 weeks prior to the Stromboli 2019 paroxysm
- High CO_2 concentrations, elevated CO_2/S_t, and negative $\delta^{13}C$ may precede paroxysms on timescales of months to weeks

Abstract

Carbon dioxide is a key gas to monitor at volcanoes because its fluctuation relative to other gases can be detected prior to eruptions, yet carbon isotopic fluctuations at volcanic summits are not well constrained. Here, we present carbon isotopes measured from plume samples collected at Stromboli volcano, Italy, by Uncrewed Aerial System (UAS). We found contrasting volcanic source $\delta^{13}C$ in 2018 during quiescence (-0.36 ± 0.59 ‰) versus 10 days before the July 3rd 2019 paroxysm (-5.01 ± 0.56 ‰). During the buildup to the eruption, an influx of CO_2-rich magma began degassing at deep levels (~100 MPa) in an open system fashion, causing strong isotopic fractionation and maintaining high CO_2/S_t ratios in the gas. This influx occurred between 10 days prior to the event and up to several months beforehand, meaning that isotopic changes in the gas could be detected weeks to months before unrest.

Plain Language Summary

Volcanoes produce gases which change composition depending on how active the volcano is. One of these gases, carbon dioxide, is known to change relative to other gases before an eruption occurs, but little is known about how the isotopes of carbon change leading up to an eruption.

Using drones to reach the gaseous plume of Stromboli volcano, Italy, we have captured carbon dioxide both during an inactive phase in 2018 and during the lead-up to a highly explosive eruption called a paroxysm. There is a stark difference in the carbon isotopes measured 10 days before the July 3rd 2019 paroxysm as opposed to those measured in 2018. This is caused by the arrival of CO_2-rich magma which progressively degassed, leading to more negative carbon isotopes in the residual magma over time. This process could have started anywhere from 10 days to several months before the paroxysm. This provides a warning signal which can be picked up weeks to months before an active period begins.

1 Introduction

Volcanoes play a significant role in the global cycle of carbon (Burton et al., 2013; Mather, 2015; Werner et al., 2019). This is because carbon is the second major species dissolved in a magma, it is transferred from the lithosphere to the atmosphere during eruption, and more significantly, during quiescence between eruptions at open-vent volcanoes (Edmonds et al., 2022). At the surface, this transfer of carbon takes the form of carbon dioxide emissions which can seep out through the ground as soil gas, dissolve into groundwater in a hydrothermal system, or be expelled from a volcanic vent. The concentration relative to other gas species (gas ratios) and flux of these CO_2 emissions can provide valuable information to understand and forecast eruptions (Aiuppa et al., 2007; Moor et al., 2016; Rizzo et al., 2009). Carbon isotopes provide information complementary to gas ratios and fluxes, as the isotopes can be used to constrain degassing models (Barry et al., 2014; Boudoire et al., 2018; Gerlach & Taylor, 1990), fingerprint the source of a magma (Fischer et al., 2015; Paonita et al., 2012; Troll et al., 2012), and monitor hydrothermal systems (D'Arcy et al., 2022; Federico et al., 2008a).

Sampling of volcanic plumes provides a safe and fast alternative to direct sampling which bypasses the need to access the crater. Depending on the topography and wind conditions, the plume can be sampled several metres to hundreds of metres away from the source vent. Methods for sampling volcanic plumes for $\delta^{13}CO_2$ analysis have undergone several advances in the last two decades. Samples were first obtained by physically entering the plume and manually collecting samples (Chiodini et al., 2011) before evolving to plume traverses in ground vehicles (Rizzo et al., 2015), helicopters (Fischer & Lopez, 2016), and use of proximal satellite laboratories (Malowany et al., 2017; Schipper et al., 2017). This field of study has entered a new era with the

onset of compact sensor arrays combined with lightweight pumps for targeted sampling of volcanic plumes by Unoccupied Aerial Systems (UAS) (D'Arcy et al., 2022; Liu et al., 2020; Shingubara et al., 2021; Tsunogai et al., 2022). These studies have demonstrated the utility of UAS in volcanic carbon isotope geochemistry, highlighting the need to continue exploring this technique.

Stromboli volcano is part of the Aeolian arc of volcanoes in Italy, which results from the subduction of the African plate below that of European (e.g. Gasparini et al., 1982). It has a well-studied volatile output, with up to ~35 mol% CO_2 during passive degassing and up to 54 mol% CO_2 during syn-explosive degassing (Aiuppa et al., 2010; Burton et al., 2007; Pering et al., 2020). Carbon isotopes at the summit of Stromboli varies from -1.0 to -2.5 ‰ $\delta^{13}CO_2$ (Capasso et al., 2005; Federico et al., 2008; Finizola et al., 2003; Di Martino et al., 2021; Rizzo et al., 2009) however gas emissions during and immediately prior to paroxysms are not so well constrained (Aiuppa et al., 2010, 2021).

In this work, we have refined a series of bespoke UAS gas sampling assemblies to collect CO_2 from a volcanic plume at Stromboli volcano, Italy, for isotopic analysis. We demonstrate that there are distinct differences between the stable carbon isotopic signature of volcanic CO_2 collected from passive degassing (quiescent periods, ground samples) compared to the CO_2 signature collected from active vents immediately prior to a devastating explosive paroxysm. This study demonstrates the potential utility of carbon isotopes to better understand open and closed degassing processes, which has implications for eruption forecasting at open-vent volcanoes.

2 Materials and Methods

2.1 Sampling and isotopic analysis

We conducted 25 sampling flights in May 2018 and June 2019 at the summit of Stromboli. We used a series of UAS (Figure 1a and 1b) and Compact Aerial Receiver-initiated Gas-sampling Operations (CARGOs) which we developed over the course of this study and which are described in detail in the Supporting Information (Text S1). Each sampling flight collected two to ten 600ml bags of volcanic gas. Bags were closed with clamps upon landing the aircraft and immediately taken from the summit to the field lab at the end of the day for same-day $\delta^{13}C$ analysis (Supporting Information Text S2-S6).

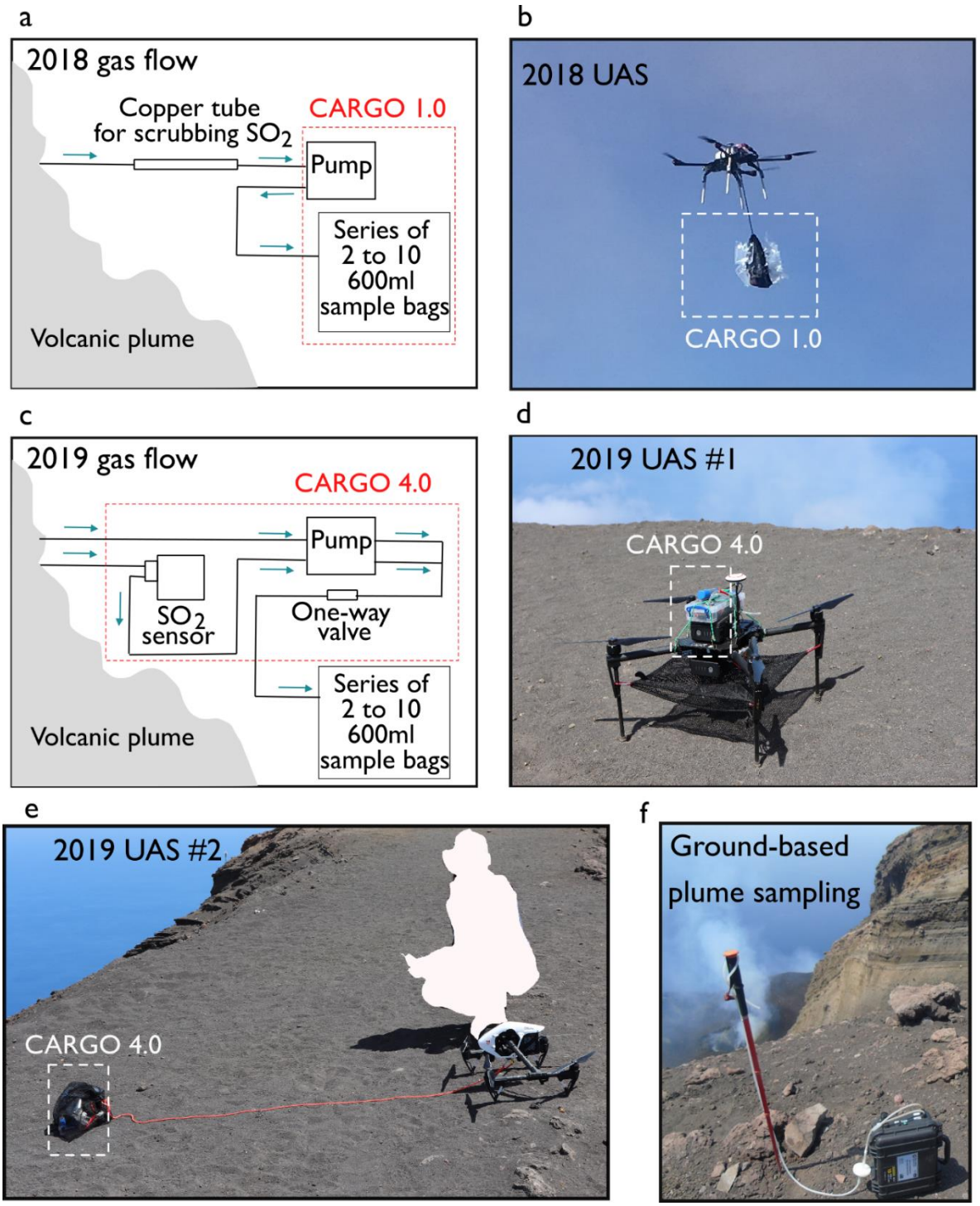

Figure 1: Sampling set-up for 2019 and 2018 samples. Gas flow schematics of the 2018 (a) and 2019 (c) Compact Aerial Receiver-initiated Gas-sampling Operations (CARGOs) along with the Uncrewed Aerial System (UAS) used to fly them in 2018 (b) and in 2019 (d, e). In (f), the general method used for ground-based sampling is pictured.

2.2 Estimates of the isotopic signature of magmatic carbon

Volcanic plumes are a mixture of atmosphere and volcanic gas, such that:

$$[\mathrm{CO_2}]_p = \mathrm{f}[\mathrm{CO_2}]_v + (1-\mathrm{f})[\mathrm{CO_2}]_b \quad [1]$$

Where f is the relative contribution from the volcanic source (Chiodini et al., 2011), and subscripts p, b, and v denote plume, background, and volcanic, respectively. To estimate the isotopic composition of the volcanic source of gas, isotopic results of plume samples must account for the presence of background air. A number of authors (Rizzo et al., 2014, 2015; Fischer and Lopez, 2016; Malowany et al., 2017; Liu et al., 2020; Shingubara et al., 2021; Tsunogai et al., 2022) have adopted the Keeling method (Keeling, 1958) to calculate the carbon signature of volcanic plumes. This method uses a linear regression analysis to fit the observations to a line of best fit, wherein one endmember is background air and the other is the volcanic source. The intercept of this line represents the theoretical composition of the volcanic source, $\delta^{13}CO_{2,v}$, when considering the variation in plume $\delta^{13}C$ against 1/ CO_2:

$$\delta^{13}\mathrm{C}_p = \frac{1}{[\mathrm{CO_2}]_p}\,[\mathrm{CO_2}]_b\,[\delta^{13}\mathrm{C_b} - \delta^{13}\mathrm{C_v}] + \delta^{13}\mathrm{C_v} \quad [2]$$

$$\delta^{13}\mathrm{C_p} = \mathrm{m}\frac{1}{[CO_2]_p} + b \quad [3]$$

There is another simplified method adapted from equation [1] which uses each discrete point sampled in a plume to estimate the $\delta^{13}CO_{2,v}$ which takes the weighted mean of the combined estimates (Schipper et al., 2017):

$$[CO_2]_v \cdot \delta^{13}\mathrm{C_v} = [CO_2]_p \cdot \delta^{13}\mathrm{C_p} - CO_{2_b} \cdot \delta^{13}\mathrm{C_b} \quad [4]$$

We applied both methods to calculate the volcanic source $\delta^{13}CO_2$.

3 Results and Discussion

3.1 Aerial samples of volcanic CO_2 capture a unique data set

The concentration of CO_2 collected during 14 flights from 12 - 17 May 2018 ranged from 405 to 490 ppmv and $\delta^{13}C$ between -7.5 and -9.2 ‰ (Supporting Information Dataset S1). The first two days of measurements were discarded due to inclement weather, which inhibited targeted flights into the plume. We also collected 16 dilute plume samples on the crater rim with a pump and portable Multi-GAS to monitor for SO_2 (indicating the volcanic plume was reaching the rim).

These ground samples varied from 410 to 463 ppm CO_2 with $\delta^{13}C$ of -7.6 to -9.0 ‰. One sample was discarded due to soil gas contamination as indicated by high CO_2 and low SO_2. Average background from 9 samples taken at the summit was 401 ppm and -8.9 ‰.

During 11 flights from 17 - 21 June 2019, we measured CO_2 concentrations ranging from 403 to 555 ppm and $\delta^{13}C$ between -8.3 and -9.8 ‰ (Dataset S1). Two samples were discarded due to leaks during a failed landing. We also collected 12 samples on the rim ranging from 408 to 501 ppm CO_2 with $\delta^{13}C$ -7.8 to -9.7 ‰. Two ground samples were discarded due to soil gas contamination. Average background from 4 samples taken at the summit was 401 ppm and -9.9 ‰.

Our sampling concentrations are comparable to those collected by UAS at other volcanoes. Shingubara et al. (2021) achieved 531 ppm (maximum volcanic CO_2 of 61 ppm), while Tsunogai et al. (2022) reached 514 ppm (maximum volcanic CO_2 of 98 ppm) at Aso volcano in Japan. At Manam volcano in Papua New Guinea, plume samples from Liu et al. (2021) ranged from 421 to 494 ppm (maximum volcanic CO_2 of 85 ppm). At Poás volcano, D'Arcy et al. (2022) reached up to 528 ppm or 120 ppm volcanic CO_2. The variation in average background at Stromboli between 2018 and 2019 samples has also been seen by workers elsewhere (Tsunogai et al., 2022) due to interferences from various sources and sinks of CO_2 around the crater.

First, the $\delta^{13}CO_{2\ volcanic}$ estimated from the Keeling method for May 2018 and June 2019 are -0.36 ± 0.59 ‰ (R^2 = 0.67, p= 0.05, n=50) and -5.01 ± 0.56 ‰ (R^2 = 0.73, p= 0.05, n=51), respectively. Errors are reported as the standard error of the regression multiplied by 1.96 to give ±2σ (Figure 2). The estimates for the weighted mean method for 2018 and 2019 using samples with volcanic CO_2 concentration greater than 50 ppm are -0.78 ± 1.34 ‰ and -4.12 ± 1.71 ‰, respectively (Dataset S2).

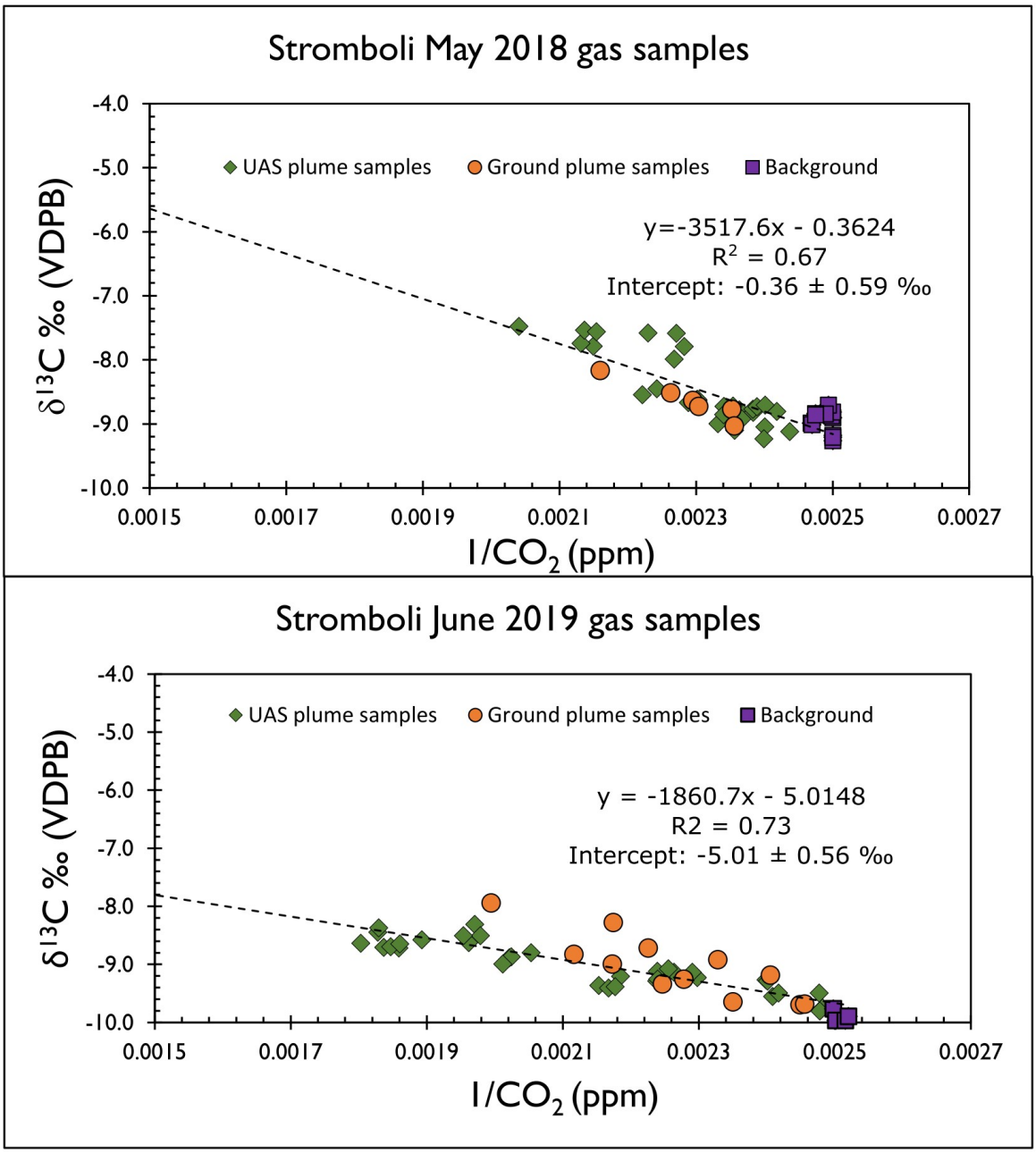

Figure 2: Stable carbon values against inverse CO_2 concentrations of all plume samples during this study. UAS (green diamonds), ground (orange circles), and background (purple squares) samples are plotted and included in a linear regression analysis whose line of best fit (dashed line) is shown for 2018 (a) and 2019 (b). This line represents a mixing line between the volcanic source and background air which is extrapolated to the y-intercept in order to estimate the $\delta^{13}CO_2$ of the high concentration volcanic source.

The volcanic source we estimate for 2018 (-0.36 ± 0.59 ‰) falls slightly outside of the range of $\delta^{13}CO_2$ measured in summit fumaroles (-1.0 to -2.5 ‰) in previous years (Figure 3). The difference in 2018 may be due to uncertainties in estimating $\delta^{13}C$, vent-specific differences, or daily variations. Significantly, the volcanic source in 2019 (-5.01 ± 0.56 ‰) is more than 2‰ more negative than the lowest $\delta^{13}C$ values usually measured at Stromboli in fumaroles (Figure 3). The large difference between the 2018 and 2019 isotopic signatures in the carbon dioxide sampled at Stromboli is a key finding, as the 2019 samples were collected two weeks prior to the July 3rd paroxysm, which was an unusually intense and fatal volcanic explosion (Andronico et al., 2021; Giordano & De Astis, 2021; Ripepe et al., 2021).

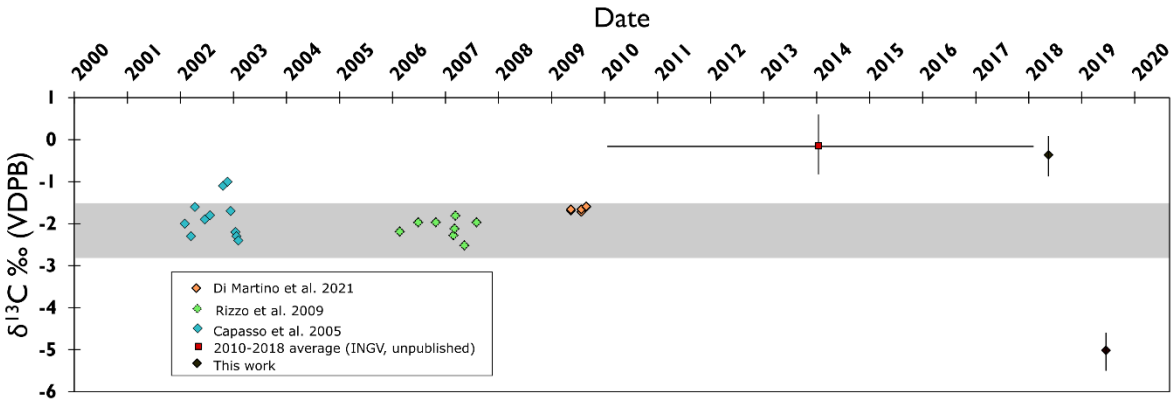

Figure 3: carbon isotopes plotted against time on the x-axis, showing where 2018 and 2019 results compare with previous studies. The grey band represents the first gas exsolved from a melt having -2.5 per mil (e=+3 and f=1). The 2010-2018 average was calculated using a regression on passive gas samples taken at the summit (n=49) with 4 blanks as background.

3.2 Carbon isotopes reveal changes prior to paroxysmal activity

The significant difference in the $\delta^{13}CO_2$ of the volcanic plume between 2018 (-0.36 ‰) and 2019 (-5.01‰) is the first of its kind measured at Stromboli. Not only has the bulk plume itself not been sampled before, but such a variation in $\delta^{13}C$ has never been observed in any fumarolic or hydrothermal sample. We posit that this is due to the unique conditions which allowed us to sample the plume close to the vent (a) during a quiescent period and (b) just two weeks before a highly energetic paroxysmal eruption which the system had been primed for. Our analytical procedures using two different instruments and employing two different statistical methods demonstrate that these results represent true volcanic variations.

The most intuitive explanation for the nearly 5 ‰ difference is a new magmatic source supplying the 2019 eruption. There are two main reasons why this appears not to be the case. Firstly, the major and trace element geochemistry of the 2019 eruptive products (Andronico et al., 2021; Métrich et al., 2021; Petrone et al., 2022) is indistinguishable from that of pyroclastic materials erupted during other recent paroxysms on Stromboli in 2003 and 2007 (Métrich et al., 2005, 2009), in which occasions fumarole direct sampling has found a stable, isotopically heavy carbon isotopic signature (Figure 3). This indicates that all these events (2003, 2007 and 2019) were charged by similar magma sourced by the same metasomatically altered mantle source (Peccerillo & Frezzotti, 2015). Secondly, there is no evidence for a magma source in the region with a $\delta^{13}CO_2$ as light as our 2019 data (-5.01 ‰). Studies from fumarolic emissions of volcanoes in the Aeolian arc range from -2.5 to -1.0 ‰ at Stromboli (G. Capasso et al., 2005; Federico et al., 2008b; A. Rizzo et al., 2009) and -3.2 to +0.7 ‰ at Vulcano (Giorgio Capasso et al., 1997; Venturi et al., 2017). Thus, while the mantle source of Stromboli volcanism is admittedly heterogeneous in terms of radiogenic isotopes and trace elements (Peccerillo et al., 2013), there is no evidence for the existence of a light carbon component in the mantle, both at a local scale (Gennaro et al., 2017) and regionally.

The next plausible mechanism for this unique carbon isotopic signature is that of isotopic fractionation during degassing. Studies have shown that, during magmatic degassing, heavier ^{13}C preferentially partitions (relative to ^{12}C) into the gas phase exsolved from a degassing silicate melt, with the extent of such an enrichment being defined by an enrichment factor $\varepsilon_{vap\text{-}melt}$ (Aubaud, 2022; Javoy et al., 1978; Mattey, 1991). As a consequence, in a batch of magma ascending and decompressing through the crust, the residual carbon remaining in the melt is expected to become progressively lighter (^{13}C-depleted) upon increasing extents of degassing, and so will the gas phase exsolved at later and shallower degassing stages (Aubaud, 2022). Importantly, the extent of this progressive ^{13}C depletion of both dissolved and exsolved carbon will depend upon whether fractionation occurs in equilibrium (closed-system) or disequilibrium (open-system) conditions between melt and the exsolved gas phase (Aubaud, 2022). Hence, magma degassing in open-system (disequilibrium) conditions can lower the $\delta^{13}C$ of the resulting gas (Aubaud, 2022) to levels that could explain our 2019 gas data.

3.3 Dynamic carbon isotopes at arc volcanoes

On Stromboli, as in other open-vent volcanoes (Edmonds et al., 2022), both closed- and open-system degassing conditions can occur, and even coexist. For example, during ordinary Strombolian activity (Harris & Ripepe, 2007; Rosi et al., 2013), both quiescent and explosive degassing coexist, in which the former is interpreted as caused by shallow gas release from convectively circulating magma in the upper conduits (Allard et al., 2008) while the latter is thought to reflect rapid, separate ascent (and explosive bursting at the surface) of deeply sourced gas bubbles (Burton et al., 2007). Important in this context is that high CO_2/SO_2 ratios have typically been observed in the bulk plume (passive + explosive) before paroxysms (Aiuppa et al., 2010) and major explosions (A. Aiuppa et al., 2011). This indicates that open-system conditions prevail in such conditions, resulting in the release of deeply sourced gas that is not in equilibrium with resident shallow conduit magma.

Geochemical and geophysical evidence supports a deeply derived gas was being emitted in the months prior to the paroxysm. First, increased CO_2 concentrations and high CO_2/SO_2 ratios were noted in the plume beginning 8 months prior to the July 2019 eruption (Aiuppa et al. 2021), indicative of a deeply sourced magma. Second, elevated CO_2 flux from summit soil began in October 2018, accelerating to July 2019 as higher volatile input was supplied (Inguaggiato et al., 2020). Third, a seismic precursor to the 3 July paroxysm was noted in very long period waveforms, starting at least 1 month before the eruption, thought to be caused by vigorous (deep-sourced?) gas jetting activity sustaining the Strombolian activity (Giudicepietro et al., 2020). Modelling the Stromboli degassing behaviour as a combination of open and closed system conditions has been invoked to account for the bimodal CO_2/SO_2 gas ratios observed prior to the July 3rd paroxysm (Aiuppa et al. 2021).

We now test if a switch from closed-system to open-system degassing conditions can explain the distinct $\delta^{13}CO_2$ plume composition in 2018 and 2019 (Fig. 4). Carbon isotopic modelling of both closed and open degassing has been used in the past to relate fluid inclusions (Barry et al., 2014; Boudoire et al., 2018) and fumaroles (Gerlach and Taylor, 1990) to their magmatic sources. Here, we use the model of Gerlach and Taylor (1990) to simulate carbon isotope fractionation during degassing in both closed-system and open-system conditions (Supplmental Information). In order to estimate f, the fraction of residual carbon in the melt at each step of the degassing

path (see eq. 5-7 in the Methods), we use the Chosetto model (Moretti et al., 2003; Moretti & Papale, 2004) to simulate degassing upon decompression of a Stromboli-like parental melt (same initial conditions as in Aiuppa et al., 2010; see Supporting Information Text S7). The model also outputs, at each degassing step (e.g., at each pressure of the modelled decompression path), the CO_2/SO_2 ratios in the gas coexisting with the melt. These are plotted, along with the gas carbon isotope signature, in Figure 4.

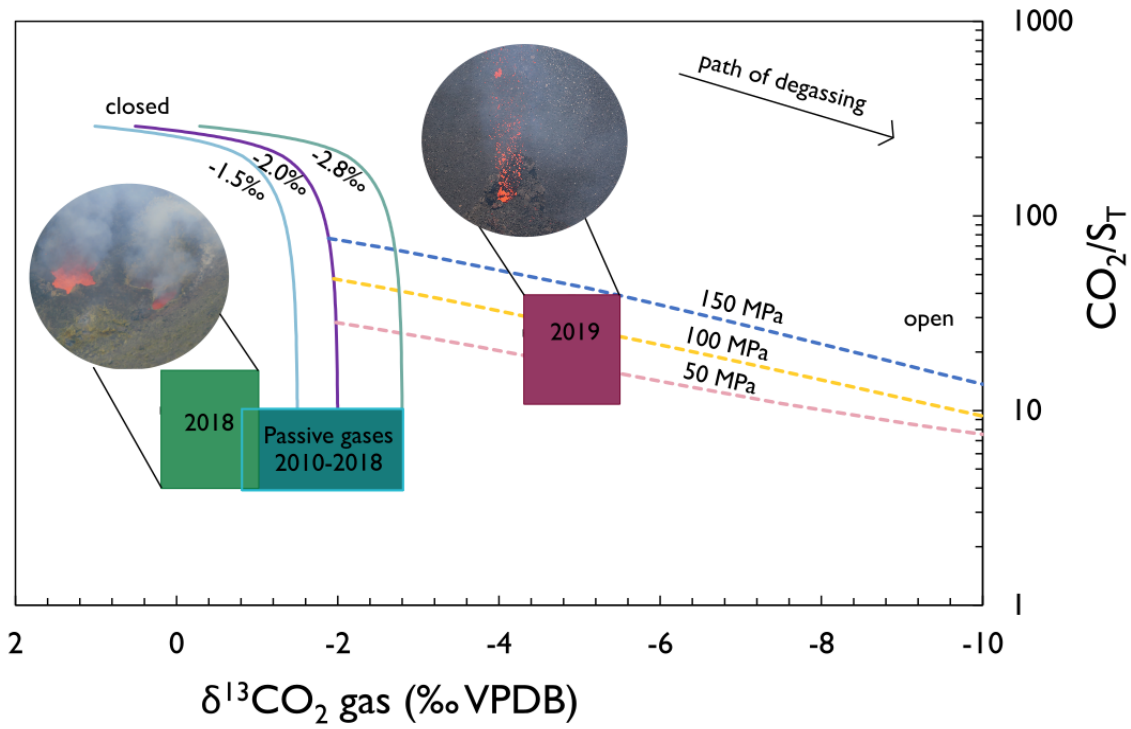

Figure 4: a) open and closed degassing paths of magma at Stromboli, showing carbon isotopic and gas ratios.

Our results indicate that the plume 2018 results, as well as the 2010-2018 fumarole data, can be explained by degassing under closed-system conditions down to 0.1 MPa (initial pressure, 1000 MPa), of a parental magma with initial $\delta^{13}CO_2$ of -0.5 to -2.8 ‰ (Figure 4). This confirms that degassing of shallow convecting magma dominates the degassing budget during ordinary Strombolian activity (Allard et al., 2008; Aiuppa et al., 2010). In contrast, we see that the 2019 plume data diverge from the closed-system degassing lines, due to their light (^{13}C-poor) carbon

signature. Our June 2019 carbon isotopic results can be reproduced from a degassing path that switches from closed to open (Figure 4). We propose a scenario in which closed-system degassing takes place as magma decompresses from 1000 MPa (~40 km) to ~50-150 MPa (2-6 km depth). At this point, magma reaches a ponding zone (a geological or rheological discontinuity), at which point accumulating gas bubbles separate from melt (Aiuppa et al., 2021), and the system switches to open degassing. Previous work has identified this transition from closed to open-system degassing based on either gas (A. Aiuppa et al., 2010; Métrich et al., 2009) evidence. This "switchover depth" from closed to open system degassing may be variable rather than constant, resulting in variable yet high CO_2/SO_2 observed before the paroxysm (~20-35). Vent-specific and short-term changes in CO_2/SO_2 were noted at Stromboli in the lead-up to the 2019 event (Pering et al., 2020). A variable switchover depth could indicate multiple levels of magma storage and/or multiple foam layers accumulating at different depths within the magma plumbing system prior to a paroxysm (Aiuppa et al., 2021). In any case, we postulate that the gas separated from the deeply accumulated magma in this open-system environment then rapidly ascends toward the surface, preserving its deeply inherited high CO_2/SO_2 ratio signature (Aiuppa et al., 2021) and also a ^{13}C-depleted isotopic signature caused by disequilibrium fractionation during open-system degassing. These are exactly the features we observe in the June 2019 plume (Figure 4).

Modern applications of carbon isotopes as monitoring tools at Stromboli assume that small increases in $\delta^{13}C$ would indicate unrest due to injection of a fresh, CO_2-rich magma (Federico et al. 2008); However, as we gain more data, it is becoming increasingly evident that this assumption may not always be true. In the same way that gas geochemists are documenting patterns of precursory CO_2/SO_2 increases prior to basaltic eruptions across many arcs (Werner et al. 2019), now is the time to build a similar repository for precursory $\delta^{13}C$ changes for Stromboli and other volcanic systems as well.

At Stromboli in 2018, the observed low CO_2/SO_2 and heavy $\delta^{13}C$ resulted from CO_2 remaining in equilibrium with the magma until shallow levels, thereby efficiently lowering the gas ratios. In 2019, high CO_2/SO_2 and light $\delta^{13}C$ were the result of the gas decoupling and separating from the deep magma at pressures of ~100 MPa. By Rayleigh fractionation, the CO_2 was depleted in ^{13}C, while CO_2/SO_2 remained relatively high. The early onset of deep gas supply many months before

the July 3rd event led to higher gas content in the deep magma reservoir which primed the magma for an energetic eruption.

4 Conclusions

What is the "recipe" for forecasting large eruptive events at Stromboli? Based on previous work (Aiuppa et al., 2021) and ours, we propose that a combination of high CO_2 concentrations (maximum volcanic CO_2 > 50 ppm) and elevated CO_2/S_t (values > 20) as measured by Multi-GAS at the summit, combined with anomalously negative $\delta^{13}C$ (e.g., less than -2 to -3 ‰), may indicate a heightened probability of a paroxysm. The longer the timescale of anomalous CO_2 characteristics, the greater the thickness of the foam layer(s) developing at depth (Aiuppa et al., 2021), hence the more powerful the eruption will be. Geophysical data may enhance this geochemical forecasting recipe. For example, (Giudicepietro et al., 2020) used seismic data to show increasing VLP size for a period of 2-4 weeks prior to the July 3rd event. In the very short-term, we can use minutes-long ground inflation detectable with tiltmeters (Ripepe et al., 2021). An integrated geochemical-geophysical approach incorporating the above parameters will improve our understanding of Stromboli and our ability to successfully forecast large eruptive events.

Our 2019 sampling was conducted two weeks prior to the July 3rd paroxysm, the largest such event for at least two decades (Bevilacqua et al., 2020). The buildup to this eruption clearly began 6-12 months beforehand (Aiuppa et al., 2021). Thus, we may have sampled at an ideal time, with maximum carbon isotopic fractionation from open system degassing. If we had sampled six months earlier, the isotopic fractionation may have been less pronounced. Likewise, other paroxysms with shorter precursory times, or major explosions which are substantially smaller than paroxysms, may produce smaller isotopic fractionations which could be more difficult to measure. We stress that the timing to forecast large paroxysmal events, whether short term (days to weeks) or longer term (weeks to months) remains unknown. Nevertheless, we hypothesize that future work may reveal systematic carbon isotopic fractionations with time if the volcano is sampled on a frequent basis, e.g., every two or three weeks. This could improve our ability to forecast both paroxysms and major explosions at Stromboli.

Acknowledgements

We thank Alfredo Alan for technical advice on the wiring schematics of the gas-sampling devices. FD is grateful for funding from Vanier Canada. JS is supported by funding from an NSERC Discovery grant. AA and ALR acknowledge funding from the Italian Ministero Ricerca e Università (PRIN projects 2017LMNLAW and 2022HA8XCS). AA also acknowledges funding from the RETURN Extended Partnership funded by the European Union Next-GenerationEU (National Recovery and Resilience Plan – NRRP, Mission 4, Component 2, Investment 1.3 – D.D. 1243 2/8/2022, PE0000005), and from Istituto Nazionale di Geofisica e Vulcanologia under research agreement "SVILUPPO DEL SISTEMA UNICO (INGV - UNIVERSITÀ) DI MONITORAGGIO VULCANICO E RILEVAMENTO PRECOCE DEI MAREMOTI E DELLE ESPLOSIONI PAROSSISTICHE DI "STROMBOLI".

Open Research

The data used in the study are available for download in the Earthchem repository (D'Arcy at al. 2024). The Chosetto code used for the CO_2 modelling was downloaded from https://github.com/charlesll/chosetto and is freely available from Github.(R. Moretti et al., 2003; Roberto Moretti & Papale, 2004).

References

Aiuppa, A., Bertagnini, A., Métrich, N., Moretti, R., Di Muro, A., Liuzzo, M., & Tamburello, G. (2010). A model of degassing for Stromboli volcano. *Earth and Planetary Science Letters*, *295*(1–2), 195–204. https://doi.org/10.1016/j.epsl.2010.03.040

Aiuppa, A., Burton, M., Allard, P., Caltabiano, T., Giudice, G., Gurrieri, S., et al. (2011). First observational evidence for the CO2-driven origin of Stromboli's major explosions. *Solid Earth*, *2*(2), 135–142. https://doi.org/10.5194/se-2-135-2011

Aiuppa, Alessandro, Moretti, R., Federico, C., Giudice, G., Gurrieri, S., Liuzzo, M., et al. (2007). Forecasting Etna eruptions by real-time observation of volcanic gas composition. *Geology*, *35*(12), 1115–1118. https://doi.org/10.1130/G24149A.1

Aiuppa, Alessandro, Burton, M., Caltabiano, T., Giudice, G., Guerrieri, S., Liuzzo, M., et al. (2010). Unusually large magmatic CO2 gas emissions prior to a basaltic paroxysm. *Geophysical Research Letters*, *37*(17), 1–5. https://doi.org/10.1029/2010GL043837

Aiuppa, Alessandro, Bitetto, M., Donne, D. D., la Monica, F. P., Tamburello, G., Coppola, D., et al. (2021). Volcanic CO2 tracks the incubation period of basaltic paroxysms. *Science Advances*, *7*(38). https://doi.org/10.1126/sciadv.abh0191

Allard, P., Aiuppa, A., Burton, M., Caltabiano, T., Federico, C., Salerno, G., & La Spina, A. (2008). Crater Gas Emissions and the Magma Feeding System of Stromboli Volcano. In *The*

Stromboli Volcano: An Integrated Study of the 2002–2003 Eruption (pp. 65–80). https://doi.org/10.1029/182gm07

Andronico, D., Del Bello, E., D'Oriano, C., Landi, P., Pardini, F., Scarlato, P., et al. (2021). Uncovering the eruptive patterns of the 2019 double paroxysm eruption crisis of Stromboli volcano. *Nature Communications*, *12*(1), 1–14. https://doi.org/10.1038/s41467-021-24420-1

Aubaud, C. (2022). Carbon stable isotope constraints on CO2 degassing models of ridge, hotspot and arc magmas. *Chemical Geology*, *605*(April), 120962. https://doi.org/10.1016/j.chemgeo.2022.120962

Barry, P. H., Hilton, D. R., Füri, E., Halldórsson, S. A., & Grönvold, K. (2014). Carbon isotope and abundance systematics of Icelandic geothermal gases, fluids and subglacial basalts with implications for mantle plume-related CO2 fluxes. *Geochimica et Cosmochimica Acta*, *134*, 74–99. https://doi.org/10.1016/j.gca.2014.02.038

Boudoire, G., Rizzo, A. L., Di Muro, A., Grassa, F., & Liuzzo, M. (2018). Extensive CO2 degassing in the upper mantle beneath oceanic basaltic volcanoes: First insights from Piton de la Fournaise volcano (La Réunion Island). *Geochimica et Cosmochimica Acta*, *235*, 376–401. https://doi.org/10.1016/j.gca.2018.06.004

Burton, M. R., Allard, P., Mure, F., & La Spina, A. (2007). Magmatic Gas Composition Reveals the Source Depth of Slug-Driven Strombolian Explosive Activity. *Science*, *317*(July), 5–8.

Burton, Michael R., Sawyer, G. M., & Granieri, D. (2013). Deep carbon emissions from volcanoes. *Reviews in Mineralogy and Geochemistry*, *75*, 323–354. https://doi.org/10.2138/rmg.2013.75.11

Capasso, G., Carapezza, M. L., Federico, C., Inguaggiato, S., & Rizzo, A. (2005). Geochemical monitoring of the 2002-2003 eruption at Stromboli volcano (Italy): Precursory changes in the carbon and helium isotopic composition of fumarole gases and thermal waters. *Bulletin of Volcanology*, *68*(2), 118–134. https://doi.org/10.1007/s00445-005-0427-5

Capasso, Giorgio, Favara, R., & Inguaggiato, S. (1997). Chemical features and isotopic composition of gaseous manifestations on Vulcano Island, Aeolian Islands, Italy: An interpretative model of fluid circulation. *Geochimica et Cosmochimica Acta*, *61*(16), 3425–3440. https://doi.org/10.1016/S0016-7037(97)00163-4

Chiodini, G., Caliro, S., Aiuppa, A., Avino, R., Granieri, D., Moretti, R., & Parello, F. (2011). First 13C/12C isotopic characterisation of volcanic plume CO2. *Bulletin of Volcanology*, *73*(5), 531–542. https://doi.org/10.1007/s00445-010-0423-2

D'Arcy, F., Aiuppa, A., Grassa, F., Rizzo, A. L., Stix, J. (2024). Volcanic gas plume isotopic ratios of carbon dioxide from Stromboli volcano, 2018-2019 [Dataset]. Version 1.0. Interdisciplinary Earth Data Alliance (IEDA). https://doi.org/10.60520/IEDA/113060.

D'Arcy, F., de Moor, J. M., Stix, J., Alan, A., Bogue, R., Corrales, E., et al. (2022). New insights into carbon isotope systematics at Poás volcano, Costa Rica. *Journal of Volcanology and Geothermal Research*, *431*(July). https://doi.org/10.1016/j.jvolgeores.2022.107639

Edmonds, M., Liu, E. J., & Cashman, K. (2022). Open-vent volcanoes fuelled by depth-integrated magma degassing. *Bulletin of Volcanology*, *84*(28). https://doi.org/10.1007/s00445-021-01522-8

Federico, C., Brusca, L., Carapezza, M. L., Cigolini, C., Inguaggiato, S., Rizzo, A., & Rouwet, D. (2008a). Geochemical Prediction of the 2002 – 2003 Stromboli Eruption From Variations in CO 2 and Rn Emissions and in Helium and Carbon Isotopes. In *The Stromboli Volcano: An Integrated Study of the 2002–2003 Eruption* (pp. 117–128).

Federico, C., Brusca, L., Carapezza, M. L., Cigolini, C., Inguaggiato, S., Rizzo, A., & Rouwet, D. (2008b). Geochemical Prediction of the 2002 – 2003 Stromboli Eruption From Variations in CO 2 and Rn Emissions and in Helium and Carbon Isotopes. In S. Calvari, S. Inguaggiato, G. Puglisi, M. Ripepe, & M. Rosi (Eds.), *The Stromboli Volcano: An Integrated Study of the 2002–2003 Eruption, Geophysical Monograph Series* (Vol. 182, pp. 117–128). Washington D.C.: American Geophysical Union.

Finizola, A., Sortino, F., Lénat, J. F., Aubert, M., Ripepe, M., & Valenza, M. (2003). The summit hydrothermal system of Stromboli. New insights from self-potential, temperature, CO2 and fumarolic fluid measurements, with structural and monitoring implications. *Bulletin of Volcanology*, *65*(7), 486–504. https://doi.org/10.1007/s00445-003-0276-z

Fischer, T P, Ramírez, C., Mora-amador, R. A., Hilton, D. R., Barnes, J. D., Sharp, Z. D., et al. (2015). Temporal variations in fumarole gas chemistry at Poás volcano , Costa Rica. *Journal of Volcanology and Geothermal Research*, *294*, 56–70. https://doi.org/10.1016/j.jvolgeores.2015.02.002

Fischer, Tobias P, & Lopez, T. M. (2016). First airborne samples of a volcanic plume for δ13C of CO2 determinations. *Geophysical Research Letters*, *43*, 3272–3279. https://doi.org/10.1002/2016GL068499.Received

Gasparini, C., Iannaccone, G., Scandone, P., & Scarpa, R. (1982). Seismotectonics of the Calabrian Arc. *Tectonophysics*, *84*, 267–286.

Gerlach, T. M., & Taylor, B. E. (1990). Carbon isotope constraints on degassing of carbon dioxide from Kilauea Volcano. *Geochimica et Cosmochimica Acta*, *54*(7), 2051–2058. https://doi.org/10.1016/0016-7037(90)90270-U

Giordano, G., & De Astis, G. (2021). The summer 2019 basaltic Vulcanian eruptions (paroxysms) of Stromboli. *Bulletin of Volcanology*, *83*(1). https://doi.org/10.1007/s00445-020-01423-2

Giudicepietro, F., López, C., Macedonio, G., Alparone, S., Bianco, F., Calvari, S., et al. (2020). Geophysical precursors of the July-August 2019 paroxysmal eruptive phase and their implications for Stromboli volcano (Italy) monitoring. *Scientific Reports*, *10*(1), 1–16. https://doi.org/10.1038/s41598-020-67220-1

Harris, A., & Ripepe, M. (2007). Temperature and dynamics of degassing at Stromboli. *Journal of Geophysical Research: Solid Earth*, *112*(3), 1–18. https://doi.org/10.1029/2006JB004393

Inguaggiato, S., Vita, F., Cangemi, M., & Calderone, L. (2020). Changes in CO2 Soil Degassing Style as a Possible Precursor to Volcanic Activity : The 2019 Case of Stromboli Paroxysmal Eruptions. *Applied Sciences*, *10*(4757). https://doi.org/doi:10.3390/app10144757

Javoy, M., Pineau, F., & Iiyama, I. (1978). Experimental determination of the isotopic fractionation between gaseous CO2 and carbon dissolved in tholeiitic magma - A preliminary study. *Contributions to Mineralogy and Petrology*, *67*(1), 35–39. https://doi.org/10.1007/BF00371631

Keeling, C. (1958). The concentration and isotopic abundances of atmospheric carbon dioxide in rural areas. *Geochimica et Cosmochimica Acta*, *13*(4), 322–334. https://doi.org/10.1016/0016-7037(58)90033-

Liu, E. J., Aiuppa, A., Alan, A., Arellano, S., Bitetto, M., Bobrowski, N., et al. (2020). Aerial strategies advance volcanic gas measurements at inaccessible, strongly degassing volcanoes. *Science Advances*, *6*(44), eabb9103. https://doi.org/10.1126/sciadv.abb9103

Malowany, K., Stix, J., de Moor, J. M., Chu, K., Lacrampe-Couloume, G., & Sherwood Lollar, B. (2017). Carbon isotope systematics of Turrialba volcano, Costa Rica, unsing a portable

cavity ring-down spectrometer. *Geochemistry, Geophysics, Geosystems*, *18*, 2769–2784. https://doi.org/10.1002/2017GC006856

Malowany, K., Stix, J., Van Pelt, A., and Lucic, G., 2015, H2S interference on CO2 isotopic measurements using a Picarro G1101-i cavity ring-down spectrometer: Atmospheric Measurement Techniques, v. 8, p. 4075–4082, doi: 10.5194/amt-8-4075-2015.

Di Martino, R. M. R., Gurrieri, S., & Camarda, M. (2021). Continous Monitoring of hydrogen and carbon dioxide at Stromboli volcano (Aeolian Islands, Italy). *Italian Journal of Geosciences*, *140*(1), 79–94. https://doi.org/10.3301/IJG.2020.26

Mather, T. A. (2015). Volcanoes and the environment: Lessons for understanding Earth's past and future from studies of present-day volcanic emissions. *Journal of Volcanology and Geothermal Research*, *304*, 160–179. https://doi.org/10.1016/j.jvolgeores.2015.08.016

Mattey, D. P. (1991). Carbon dioxide solubility and carbon isotope fractionation in basaltic melt. *Geochimica et Cosmochimica Acta*, *55*(11), 3467–3473. https://doi.org/10.1016/0016-7037(91)90508-3

Métrich, N., Bertagnini, A., Landi, P., Rosi, M., & Belhadj, O. (2005). Triggering mechanism at the origin of paroxysms at Stromboli (Aeolian Archipelago, Italy): The 5 April 2003 eruption. *Geophysical Research Letters*, *32*(10), 1–4. https://doi.org/10.1029/2004GL022257

Métrich, N., Bertagnini, A., & Di Muro, A. (2009). Conditions of magma storage, degassing and ascent at Stromboli: New insights into the volcano plumbing system with inferences on the eruptive dynamics. *Journal of Petrology*, *51*(3), 603–626. https://doi.org/10.1093/petrology/egp083

Métrich, N., Bertagnini, A., & Pistolesi, M. (2021). Paroxysms at Stromboli Volcano (Italy): Source, Genesis and Dynamics. *Frontiers in Earth Science*, *9*(February), 1–17. https://doi.org/10.3389/feart.2021.593339

Moor, J. M. De, Aiuppa, A., Pacheco, J., Avard, G., Kern, C., Liuzzo, M., et al. (2016). Short-period volcanic gas precursors to phreatic eruptions : Insights from Poás Volcano , Costa Rica. *Earth and Planetary Science Letters*, *442*, 218–227. https://doi.org/10.1016/j.epsl.2016.02.056

Moretti, R., Papale, P., & Ottonello, G. (2003). A model for the saturation of C-O-H-S fluids in silicate melts. *Geological Society Special Publication*, *213*, 81–101. https://doi.org/10.1144/GSL.SP.2003.213.01.06

Moretti, Roberto, & Papale, P. (2004). On the oxidation state and volatile behavior in multicomponent gas-melt equilibria. *Chemical Geology*, *213*(1–3), 265–280. https://doi.org/10.1016/j.chemgeo.2004.08.048

Paonita, A., Caracausi, A., Iacono-Marziano, G., Martelli, M., & Rizzo, A. (2012). Geochemical evidence for mixing between fluids exsolved at different depths in the magmatic system of Mt Etna (Italy). *Geochimica et Cosmochimica Acta*, *84*, 380–394. https://doi.org/10.1016/j.gca.2012.01.028

Peccerillo, A., & Frezzotti, M. L. (2015). Magmatism, mantle evolution and geodynamics at the converging plate margins of Italy. *Journal of the Geological Society*, *172*(4), 407–427. https://doi.org/10.1144/jgs2014-085

Peccerillo, A., De Astis, G., Faraone, D., Forni, F., & Frezzotti, M. L. (2013). Compositional variations of magmas in the aeolian arc: Implications for petrogenesis and geodynamics. In F. Lucchi, A. Peccerillo, T. Keller, C. Tranne, & P. Rossi (Eds.), *The Aeolian Island*

Volcanoes (Memoirs, Vol. 37, pp. 491–510). London: Geological Society. https://doi.org/10.1144/M37.15

Pering, T. D., Liu, E. J., Wood, K., Wilkes, T. C., Richardson, T., Mcgonigle, A. J. S., & Aiuppa, A. (2020). Combined ground and aerial measurements resolve vent-specific gas fluxes from a multi-vent volcano. *Nature Communications*. https://doi.org/10.1038/s41467-020-16862-w

Petrone, C. M., Mollo, S., Gertisser, R., Buret, Y., Scarlato, P., Del Bello, E., et al. (2022). Magma recharge and mush rejuvenation drive paroxysmal activity at Stromboli volcano. *Nature Communications*, *13*(1), 1–17. https://doi.org/10.1038/s41467-022-35405-z

Ripepe, M., Lacanna, G., Pistolesi, M., Silengo, M. C., Aiuppa, A., Laiolo, M., et al. (2021). Ground deformation reveals the scale-invariant conduit dynamics driving explosive basaltic eruptions. *Nature Communications*, *12*(1). https://doi.org/10.1038/s41467-021-21722-2

Rizzo, A., Grassa, F., Inguaggiato, S., Liotta, M., Longo, M., Madonia, P., et al. (2009). Geochemical evaluation of observed changes in volcanic activity during the 2007 eruption at Stromboli (Italy). *Journal of Volcanology and Geothermal Research*, *182*(3–4), 246–254. https://doi.org/10.1016/j.jvolgeores.2008.08.004

Rizzo, A. L., Liuzzo, M., Ancellin, M. A., & Jost, H. J. (2015). Real-time measurements of δ13C, CO2 concentration, and CO2/SO2 in volcanic plume gases at Mount Etna, Italy, over 5 consecutive days. *Chemical Geology*, *411*, 182–191. https://doi.org/10.1016/j.chemgeo.2015.07.007

Rizzo, Andrea Luca, Jost, H. J., Caracausi, A., Paonita, A., Liotta, M., & Martelli, M. (2014). Real-time measurements of the concentration and isotope composition of atmospheric and volcanic CO2 at Mount Etna (Italy). *Geophysical Research Letters*, *41*(April), 2382–2389. https://doi.org/10.1002/2014GL059722

Rosi, M., Pistolesi, M., Bertagnini, A., Landi, P., Pompilio, M., & Di Roberto, A. (2013). Stromboli volcano, Aeolian Islands (Italy): Present eruptive activity and hazards. *Geological Society Memoir*, *37*(1), 473–490. https://doi.org/10.1144/M37.14

Schipper, C. I., Moussallam, Y., Curtis, A., Peters, N., Barnie, T., Bani, P., et al. (2017). Isotopically (δ13C and δ 18 O) heavy volcanic plumes from Central Andean volcanoes: a field study. *Bulletin of Volcanology*, *79*(8). https://doi.org/10.1007/s00445-017-1146-4

Shingubara, R., Tsunogai, U., Ito, M., Nakagawa, F., Yoshikawa, S., Utsugi, M., & Yokoo, A. (2021). Development of a drone-borne volcanic plume sampler. *Journal of Volcanology and Geothermal Research*, *412*, 107197. https://doi.org/10.1016/j.jvolgeores.2021.107197

Troll, V. R., Hilton, D. R., Jolis, E. M., Chadwick, J. P., Blythe, L. S., Deegan, F. M., et al. (2012). Crustal CO2 liberation during the 2006 eruption and earthquake events at Merapi volcano , Indonesia. *Geophysical Research Letters*, *39*, 1–6. https://doi.org/10.1029/2012GL051307

Tsunogai, U., Shingubara, R., Morishita, Y., Ito, M., Nakagawa, F., Yoshikawa, S., et al. (2022). Sampling Volcanic Plume Using a Drone-Borne SelPS for Remotely Determined Stable Isotopic Compositions of Fumarolic Carbon Dioxide. *Frontiers in Earth Science*, *10*(March), 1–12. https://doi.org/10.3389/feart.2022.833733

Venturi, S., Tassi, F., Bicocchi, G., Cabassi, J., Capecchiacci, F., Capasso, G., et al. (2017). Fractionation processes affecting the stable carbon isotope signature of thermal waters from hydrothermal / volcanic systems : The examples of Campi Flegrei and Vulcano Island (southern Italy). *Journal of Volcanology and Geothermal Research*, *345*, 46–57. https://doi.org/10.1016/j.jvolgeores.2017.08.001

Werner, C., Fischer, T. P., Aiuppa, A., Edmonds, M., Cardellini, C., Carn, S., et al. (2019). Carbon Dioxide Emissions from Subaerial Volcanic Regions: Two Decades in Review. In B. Orcutt, I. Daniel, & R. Dasgupta (Eds.), *Deep Carbon: Past to Present* (pp. 188–236). Cambridge: Cambridge University Press. https://doi.org/doi:10.1017/9781108677950

Geophysical Research Letters

Supporting Information for

Large isotopic shift in volcanic plume CO_2 prior to a basaltic paroxysmal explosion

Fiona D'Arcy[1], Alessandro Aiuppa[2], Fausto Grassa[3], Andrea Luca Rizzo[4,5], John Stix[1]

[1] McGill University, Montreal, Canada
[2] Dipartimento DiSTeM, Università degli Studi di Palermo, Palermo, Italy
[3] Istitutio Nazionale di Geofisica e Vulcanologia, Palermo, Palermo, Italy
[4] Department of Earth and Environmental Sciences, University of Milano-Bicocca, Piazza della Scienza 4, 20126, Milan, Italy
[5] Istitutio Nazionale di Geofisica e Vulcanologia, Sezione di Milano, Via Alfonso Corti 12, Milan, Italy

Contents of this file

Text S1 to S7
Figures S1 to S8
Caption for Dataset S1
Caption for Dataset S2

Additional Supporting Information (Files uploaded separately)

Dataset S1
Dataset S2

Introduction

The Supporting Information contains details of the methods including sampling instrumentation (Text S1), fractionation tests (Text S1), isotopic analysis and calibration (Text S1 -S4 and Figures S1-S5), comparison of regression methods of calculating the volcanic source (Text S5-S6 and Figures S6-S8), and modelling parameters and equations for the pressure- depth-carbon isotope model (Text S7). We also include captions for datasets S1 and S2 which are uploaded as separate files.

Text S1. Sampling techniques and methodology

2018 UAS and non-automated pump

This was the first attempt to capture volcanic gas samples, which was used at Stromboli in 2018. This first approach was a simple combination consisting of a 1.2 L/minute TD-3LS Brailsford® pump powered by a USB battery. The pump and battery were contained in a lightweight plastic container, with tygon tubing leading from the outlet to a 15 cm copper tube filled with copper filings to eliminate H_2S gas from being sampled, in order to reduce interference with subsequent carbon isotopic analysis as described in (Malowany et al., 2015). From the copper tube, short segments of tubing <20 cm were connected in series to two to ten 600 ml gas bags. This payload was placed into a mesh drawstring bag and suspended from a 2 metre long paracord, inspired by similar designs to capture volcanic crater water samples while keeping the UAS above the corrosive gases. This cord was attached with a carabiner to the lower frame of a TurboAce Matrix I quadcopter with a flight time of ~10 minutes. The pump was manually turned on with a switch just before take-off and turned off just after landing.

2019 UAS and CARGO 4.0

Building upon the challenges of the first test in 2018, we decided to build a new custom gas sampling system integrated with telemetry functions for the 2019 sampling campaign at Stromboli. The UAS was maneuvered with one remote controller by the pilot, while the gas sampling unit was controlled by a second person using a secondary remote controller to switch the pump on and off. The Compact Aerial Receiver-initiated Gas-sampling operation (CARGO 4.0) did not include copper tubes in order to limit excess weight for longer flight times. The other main difference is that the pump switch and SO_2 sensor were mapped to channels on a remote controller for the drone, allowing the pilot to use two-way telemetry to read the voltage of the SO_2 sensor and turn the pump on and off for sampling. The payload (700 grams) consisted of a pump (micropump®, model d3k, 2.5 L/minute) connected to an electronic switch (Turnigy 10A/30V) which utilized an empty standard port on the UAS receiver. An SO_2 sensor (Citicell 0-200 ppmv range) was included with a voltage sensor (Futaba SBS-01V) connected to the SBUS2 port of the receiver and one of the inlet tubes of the pump. A portable USB-powered charger supplied power to the pump while a 9 volt battery powered the SO_2 sensor.
The assembly was deployed with two different UAS over the course of the fieldwork; a DJI Matrice 100 on June 17-18 and a DJI Inspire on June 20. The DJI Matrice 100 (UAS #1, figure 1) had a flight time of ~20 minutes and a payload comprising the gas sampling configuration attached on top of the UAS body which was secured with bungee cords, while two to four gas sample bags were attached directly below the drone. The DJI Inspire 1 (UAS #2, figure 1) had a flight time of ~10 minutes with the payload comprising the CARGO 4.0 as a separate unit suspended 1.5 metres below the UAS in a mesh bag.

Fractionation test of the CARGO 4.0

While the first sampling technique in 2018 involved a simple tubing and pump system, the multicomponent assemblies used in 2019 required that the gas pass through an SO_2 sensor before being drawn through the pump and into sample bags (Figure 1c and 1d).

We performed a simple test to evaluate possible fractionation from gas flowing through the SO_2 sensor in the 2019 CARGO. We analyzed a gas standard (-15.6 ‰ $\delta^{13}CO_2$) before passing it through the 2019 sampling assembly and collecting the gas for subsequent measurement (supplementary material). The measured value of the standard ranged from -15.77 ± 0.44 ‰ to -15.82 ± 0.38 ‰ $\delta^{13}CO_2$ before passing through the system and from -15.66 ± 0.35 ‰ to -15.83 ± 0.43 ‰ $\delta^{13}CO_2$ after passing through the SO_2 sensor and pump. This is a difference of 0.04 ‰ between the medians of the two sets of samples, indicating that isotopic fractionation due to passage through the SO_2 sensor is negligible or non-existent, as has been shown in other similar systems (Schipper et al., 2017)

Ground-based plume sampling

Ambient plume samples were taken from the crater rim by placing the inlet tube on top of a hiking stick 1 metre above the ground and connected to a mulltiGAS sensor with continuous pumping. When the multiGAS indicated high SO_2 readings, a 600ml sample bag was connected to the outlet tube and filled.

Text S2. Isotopic analysis

The gold standard for $\delta^{13}C$ analysis is Isotope Ratio Mass Spectrometry (IRMS); however, these instruments must be kept in a stable lab environment due to their sensitivity. Rizzo et al. (2014) demonstrated that $\delta^{13}C$ studies of volcanic plumes with laser-based isotope ratio infrared spectrometers (IRIS) are feasible for harsh environments and provide comparable isotopic results to those measured by IRMS. Similarly, Malowany et al. (2017) demonstrated that a Cavity Ring-Down Spectrometer (CRDS) could be used for near real-time ^{13}C analysis of volcanic plumes. In our study, we used both an IRIS (Delta Ray from Thermo Scientific) and a CRDS (G2201-i from Picarro). We analyzed a subset of samples on each instrument by connecting sample bags to the Picarro instrument until a stable $\delta^{13}C$ signal was achieved, then detaching the bag and immediately measuring the same bag on the Delta Ray instrument. A series of standard gases was used to calibrate the Picarro instrument in 2018, and both the Picarro and Delta Ray in 2019. In 2018, the two instruments were in good agreement, with standard deviations between the same sample bag measured on each instrument never exceeding 0.4 ‰. In 2019, the standard deviations of individual measurements between the two instruments did not exceed 0.7‰, with a maximum difference of 1 ‰ between analysis of the same sample on each instrument.

All samples were analyzed within 12 hours on a Picarro G2201-i CRDS and a Thermo Scientific Delta Ray IRIS at the field station. A copper tube filled with fine copper wire cuttings was used to remove any interference from H_2S, and three in-house standards (-43.15‰, -15.6‰, and -11.4‰) were used to define a calibration curve (supplemental info). A standard was run every 5 to 12 samples at concentrations ranging from 450 to 1050 ppmv CO_2 to monitor instrumental drift. Stable carbon isotopes were calculated using delta notation, where:

$$\delta^{13}C\ (‰) = \left(\frac{\left({}^{13}C/{}^{12}C \right)_{sample}}{\left({}^{13}C/{}^{12}C \right)_{standard}} - 1 \right) \cdot 1000 \qquad [1]$$

Carbon isotopic results are reported using the per mil notation which provides values relative to the Vienna Pee Dee Belemnite (VPDB) reference standard. Repeat analysis of 8 standards shows that uncertainties are ~0.3 ‰.

Our data is unique in that we were able to perform the usual calibrations with standards brought into the field in overpressured Wheaton gas bottles, as well as compare our isotopic results across the two portable instruments (Picarro and Delta Ray) in the field. In the following section we explain how we corrected the data.

Text S3. Standards for calibration of isotopic data

The 2018 Picarro data were calibrated with 18 individual standard measurements (Figure S1). The standards were measured at the beginning of the field campaign on May 12, as well as each day before and after samples were analyzed. The standards used were -15.6 per mil, -43.15 per mil, and -11.4 per mil. The Delta Ray analyses were corrected internally by the system which uses an intake of two reference gases from gas cylinders. The difference between the corrected Picarro and Delta Ray data was less than 0.5 per mil with a standard deviation of 0.16 per mil.

The 2019 data, being a larger dataset than that of 2018 as well as having standards analyzed on both the Picarro and Delta Ray instruments, underwent an extensive calibration (Figure S2). The Picarro data were calibrated with 15 individual standard measurements. The standards were measured at the beginning of the field campaign on June 17 as well as each day before and after samples were analyzed. In addition to an internal calibration, the Delta Ray underwent a calibration with 6 standards. For both Delta Ray and Picarro, the standards used were -15.6 per mil and -43.15 per mil, while the Picarro also used three additional standards for manual calibration of -11.4 per mil, -3.88 per mil, -39.98 per mil, and -0.63 per mil. The difference between the corrected Picarro and Delta ray values was less than 1.0 per mil with a standard deviation of 0.35 per mil.

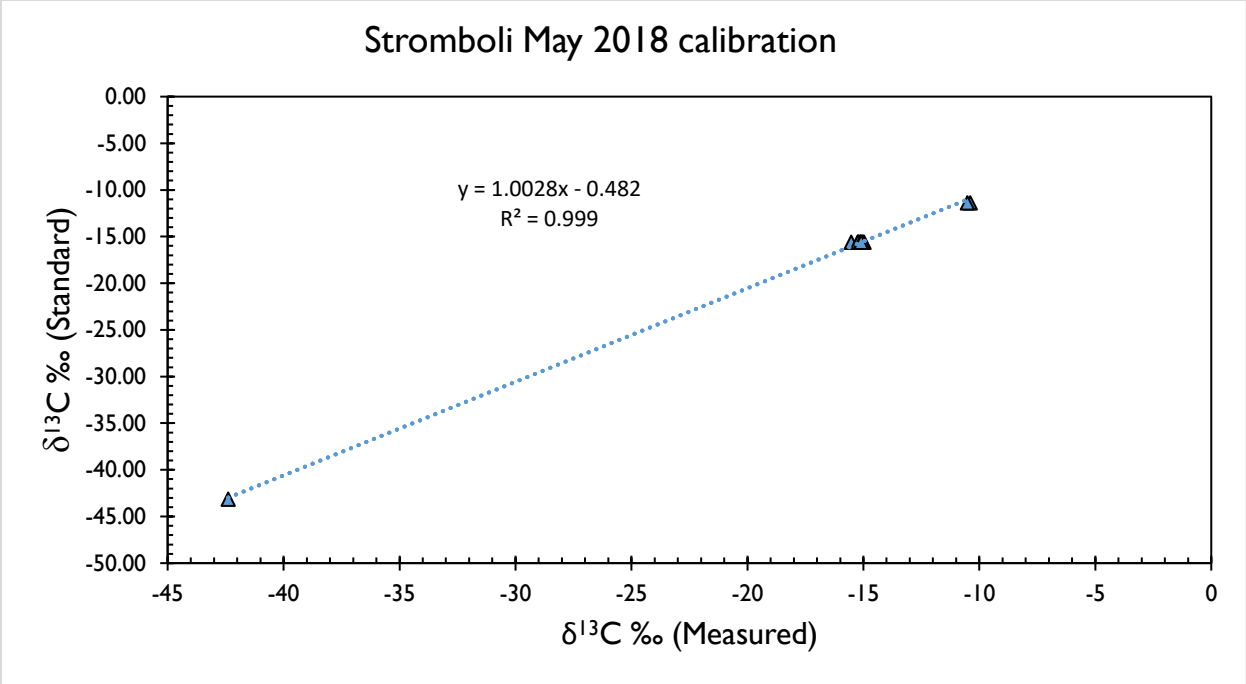

Figure S1. Calibration of 2018 standards measured on the Picarro instrument versus known standard values. The line of best fit is used to correct all Picarro data from the 2018 field campaign. The correction brought the carbon isotopic value 0.75 per mil lighter, on average.

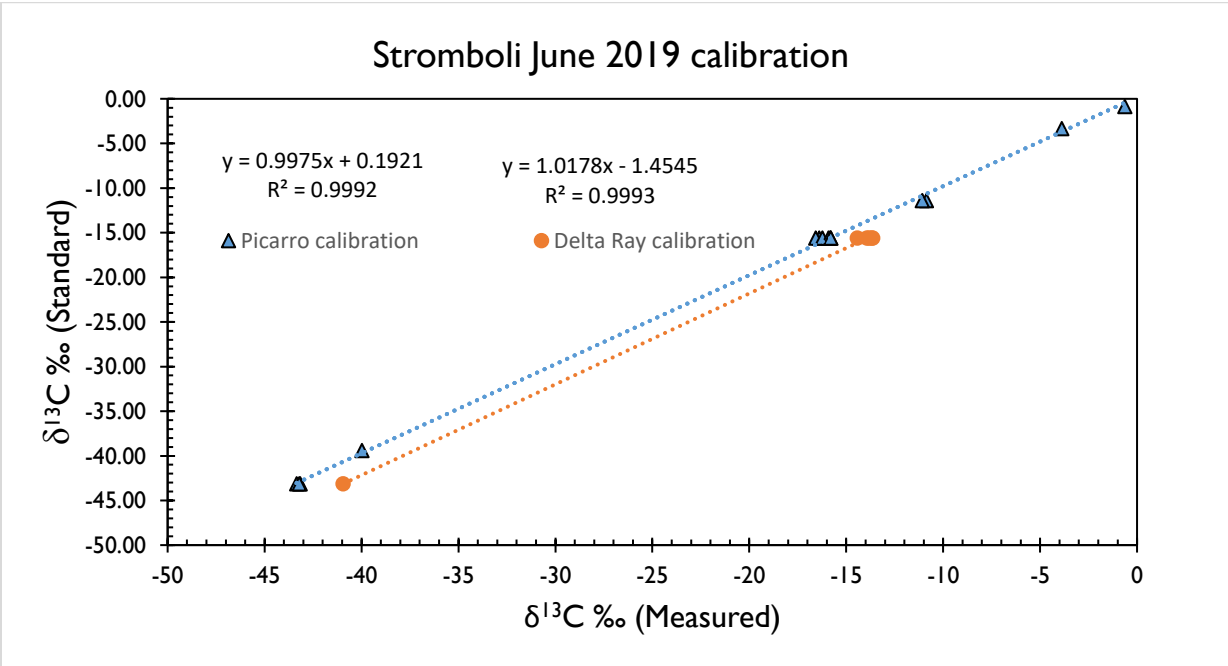

Figure S2: Calibration of 2019 standards measured on the Picarro and Delta Ray instruments versus known standard values. The orange line of best fit is used to correct all Delta Ray data and the blue line of best fit is used to correct all Picarro data from the

2018 field campaign. The correction brought the carbon isotopic value 0.2 per mil heavier for Picarro and 1.6 per mil lighter for Delta Ray, on average.

Text S4. Calibration for concentration

We also performed a test to determine if a correction for the CO_2 concentration between the two instruments was necessary. After plotting concentration for matching analyses from both instruments against each other (Figures S3, S4), we applied a correction to the Picarro dataset based on the Delta Ray concentrations. While the 2018 concentrations of equivalent samples on each instrument was a 20ppm difference on average, the correction brought the difference down to less than 4ppm. However, as we had a smaller subset of samples on the Delta Ray, this led to a coefficient of regression less than 0.5. The 2019 concentrations of equivalent samples on each instrument was a 13ppm difference on average, and the correction brought the difference down to 1ppm. Finally, when the Picarro values which were corrected for concentration were plotted together with the Delta Ray data, each dataset deviated from the other in that the intercepts were different by 4 per mil or more (Figure S5). Since we could not ascertain which instrument has more accurate concentrations, we decided to omit the correction for concentration to avoid over-processing the data. In future work, we would perform a calibration with standards of known concentration in the same way that the isotopic values were calibrated.

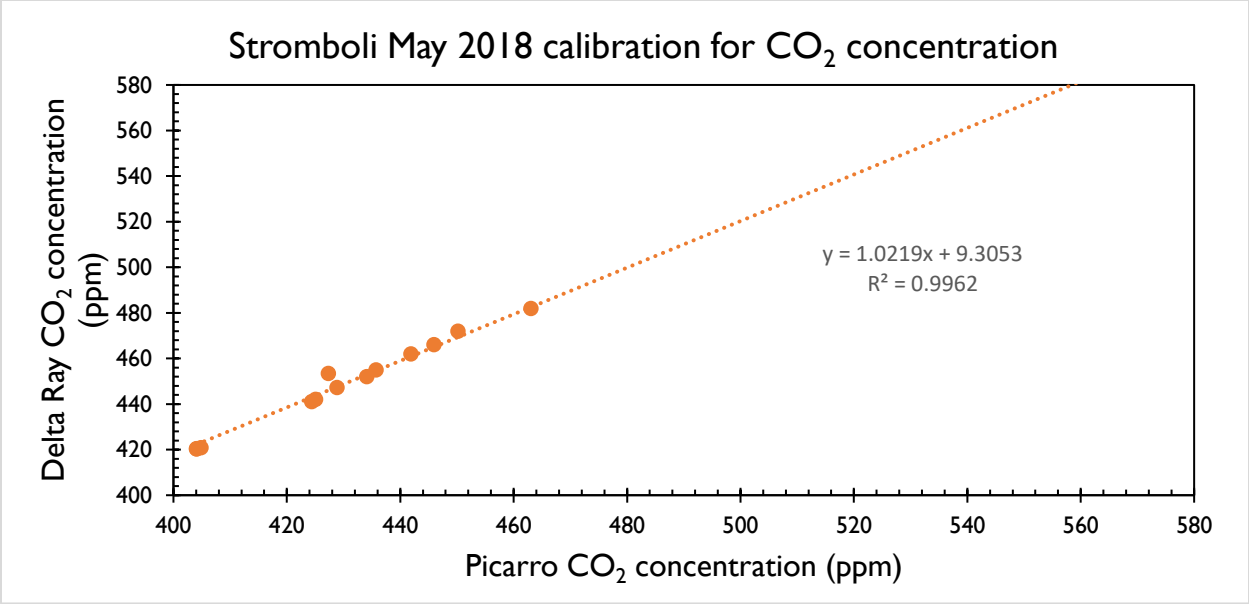

Figure S3: The Picarro versus Delta Ray concentration data for the 2018 field campaign.

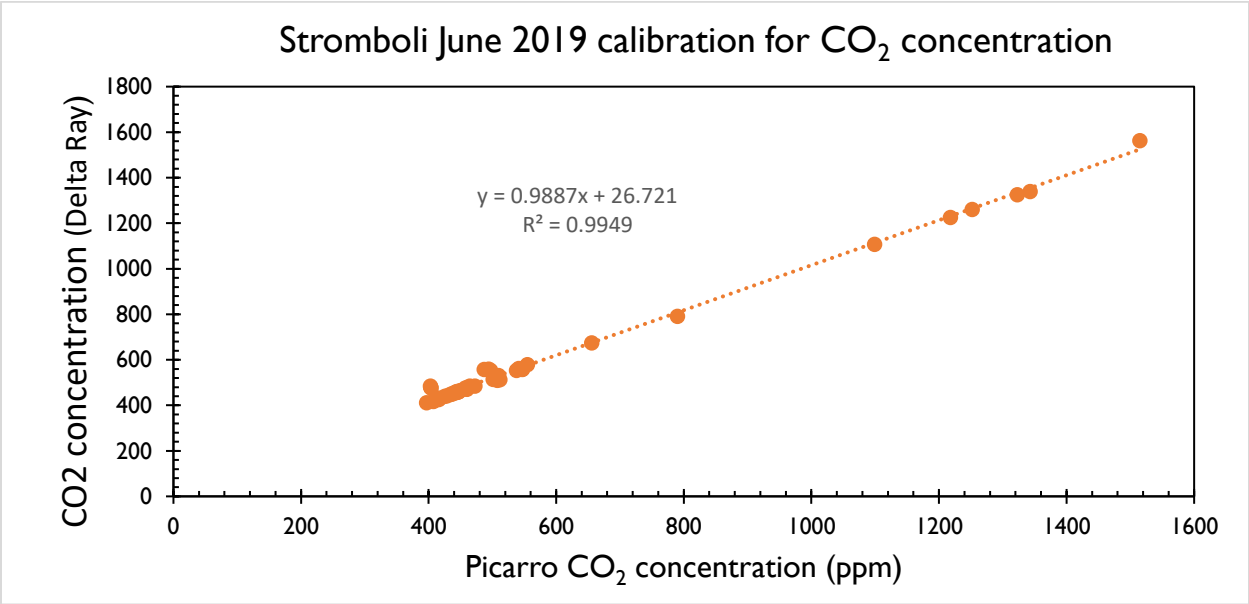

Figure S4: The Picarro versus Delta Ray concentration data for the 2019 field campaign.

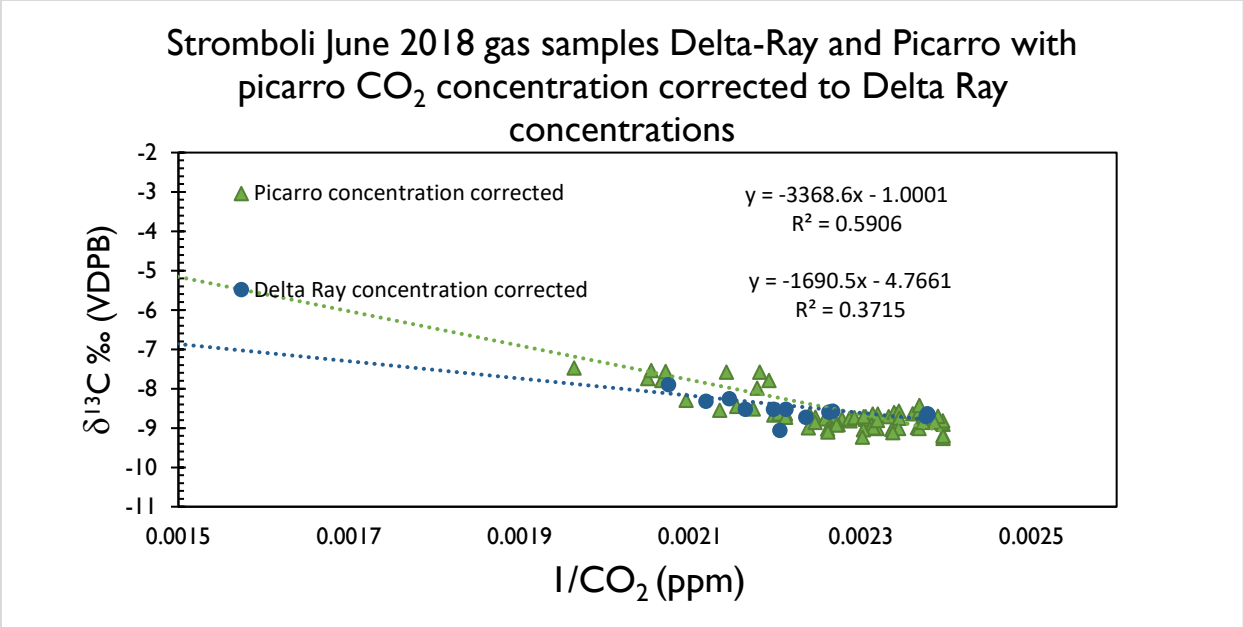

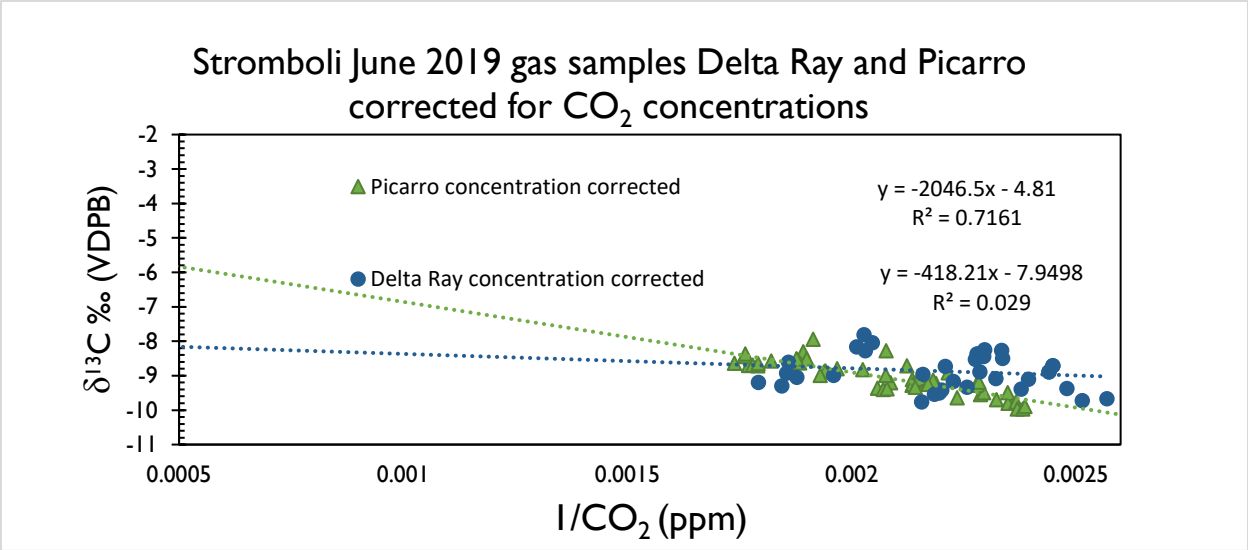

Figure S5: The Picarro and Delta Ray corrected concentration data for the 2018 (top) and 2019 (bottom) field campaigns.

Text S5. Cross calibration of regression analysis between Delta Ray and Picarro

In order to assess whether the difference between 2018 and 2019 data is significant, i.e. whether it represents a true volcanic variation in signature rather than being an artifact of the data processing, we were able to perform many tests to cross-calibrate the data between the two instruments to check the accuracy of each dataset. After calibration, differences between the two samples sets remained, which we discuss below.

The discrepancy between 2018 Delta Ray and Picarro data is likely due to the limited number of samples for a single day of measurements for the Delta Ray. This reduces the accuracy of the dataset, as can be seen by the low coefficient of regression for delta ray in

figure S6 (R2=0.37). It is possible that there were spatial and/or temporal variations at play as well. Unlike 2019, in 2018 we flew from two different take-off points to capture the samples and these flights were vent-specific. On 15 May, we flew from the pizzo targeting the C vent, which coalesces into a bulk plume at around 100 m height where plumes from several vents in the central and south crater merge. On 16 and 17 May, we flew from the helipad targeting the NE vent. While the Picarro collected samples on 15 to 17 May, the Delta Ray collected data only on 16 May. The lower intercept of the Delta Ray data (-4.8‰) is consistent with the 16 May Picarro data (Figure S7), which has a much lower intercept (-3.8‰) compared to the full Picarro dataset (-0.36‰). Furthermore, the combined Picarro and Delta Ray data for 2018 (Figure S6) shows a lower intercept (-2.0‰) than the Picarro data alone (-0.36‰), since the 16 May data are weighted towards lighter values from the additional Delta Ray samples.

The overall intercept for 2019 with Picarro data is -5.0 ‰ and a high R^2 value of 0.7, while the Delta Ray intercept is -7.8 ‰ with a R^2 of 0.03 (Figure S8). The combined data yield an intercept of -5.9 ‰ (R2= 0.3). Again, the 2019 differences between Delta Ray and Picarro are likely due to fewer analyses performed by the Delta Ray as well as a larger spread of data in the Delta Ray results.

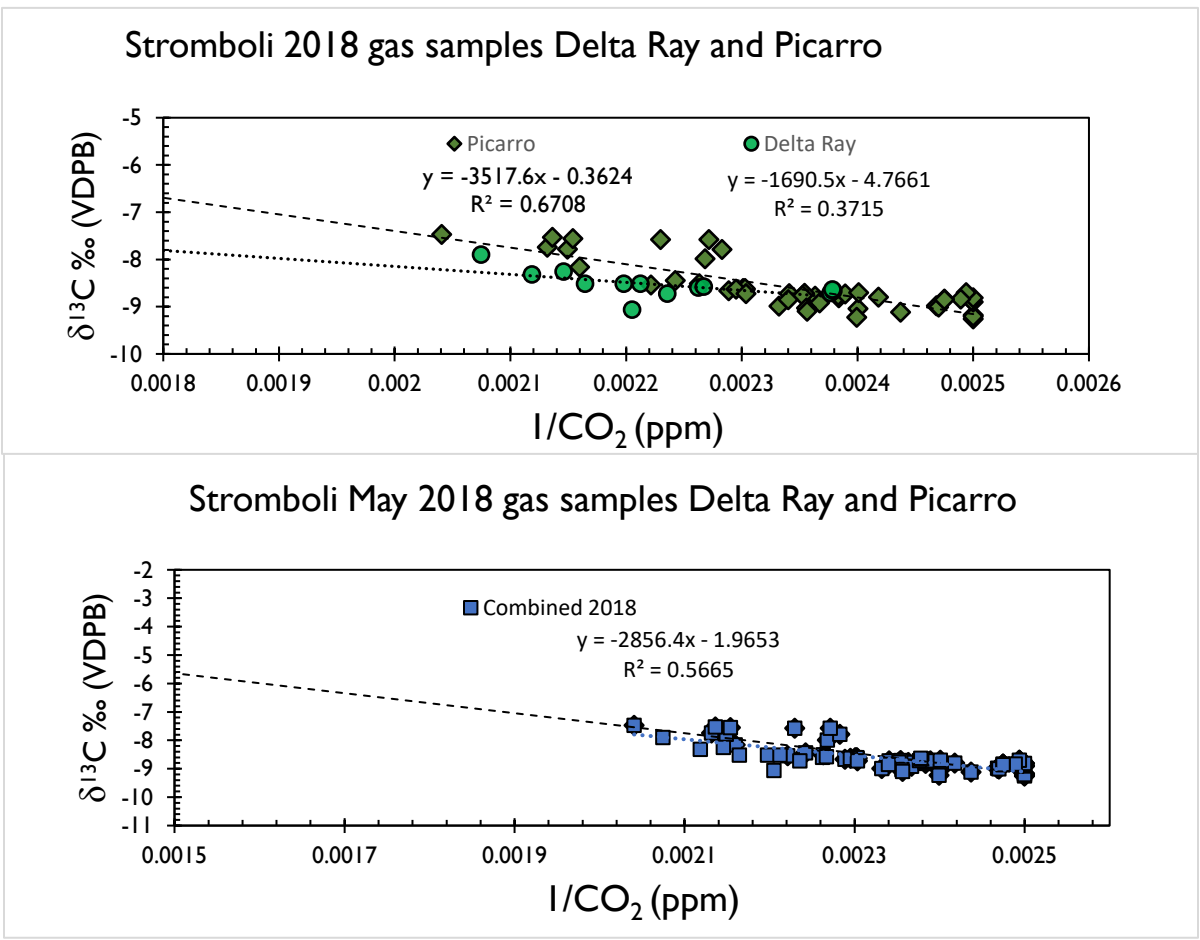

Figure S6: The Picarro and Delta Ray data for 2018 showing the datasets from both instruments plotted separately (top) and combined (bottom).

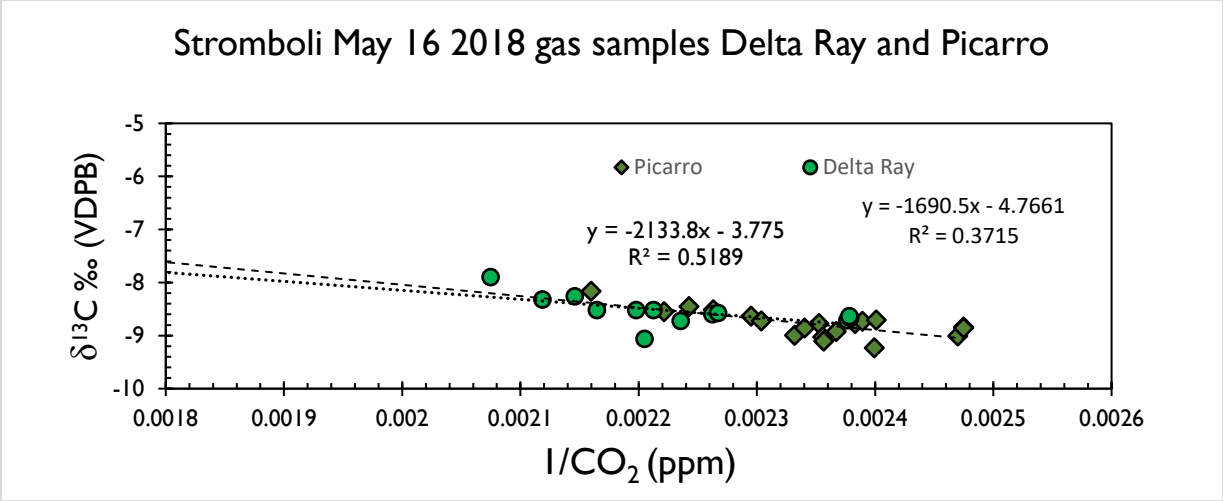

Figure S7: The Picarro and Delta Ray data for May 16 2018 showing the datasets from both instruments plotted separately. These include background, UAS flights, and ground-based plume samples.

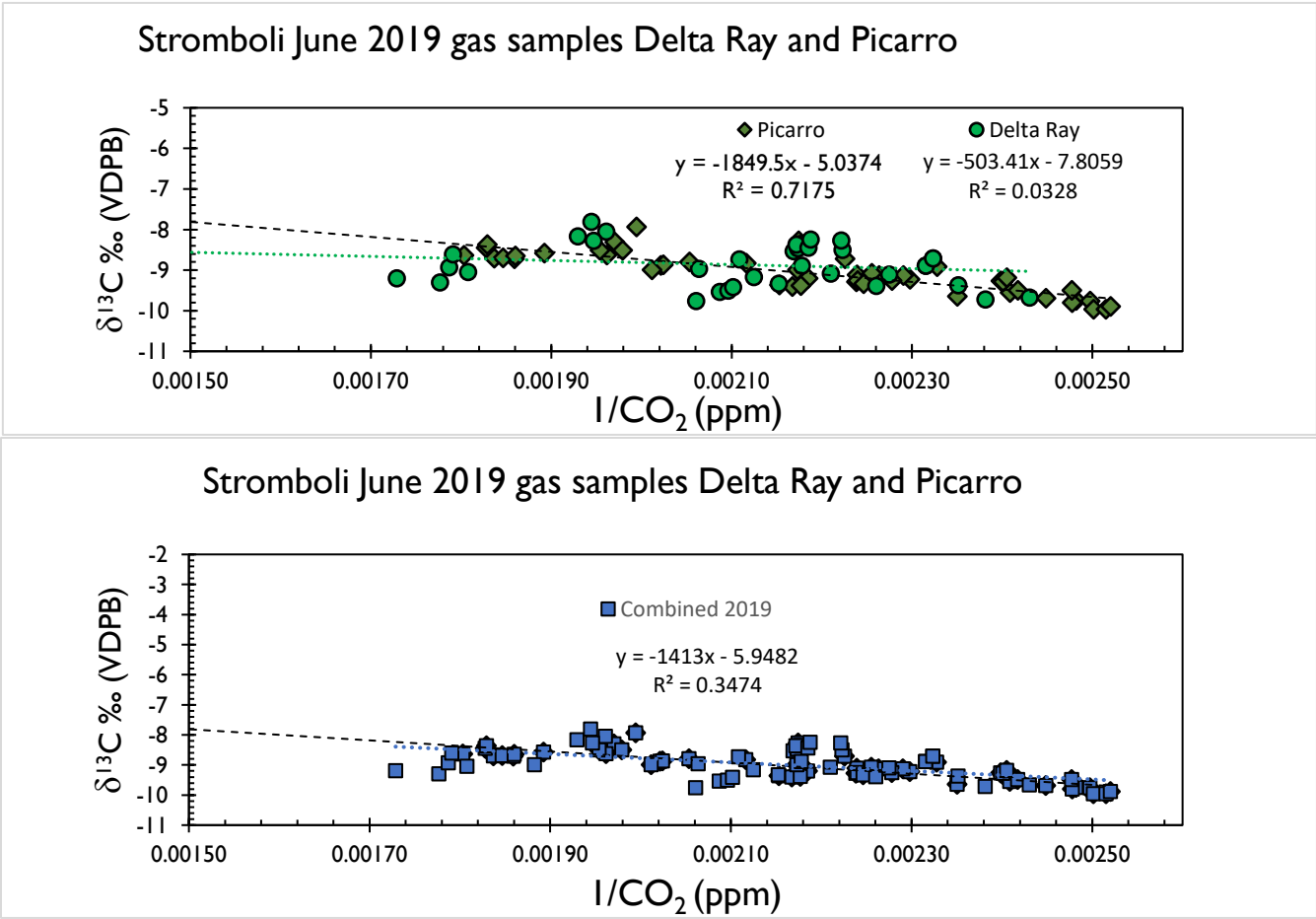

Figure S8: The Picarro and Delta Ray data for 2018 showing the datasets from both instruments plotted separately (top) and combined (bottom).

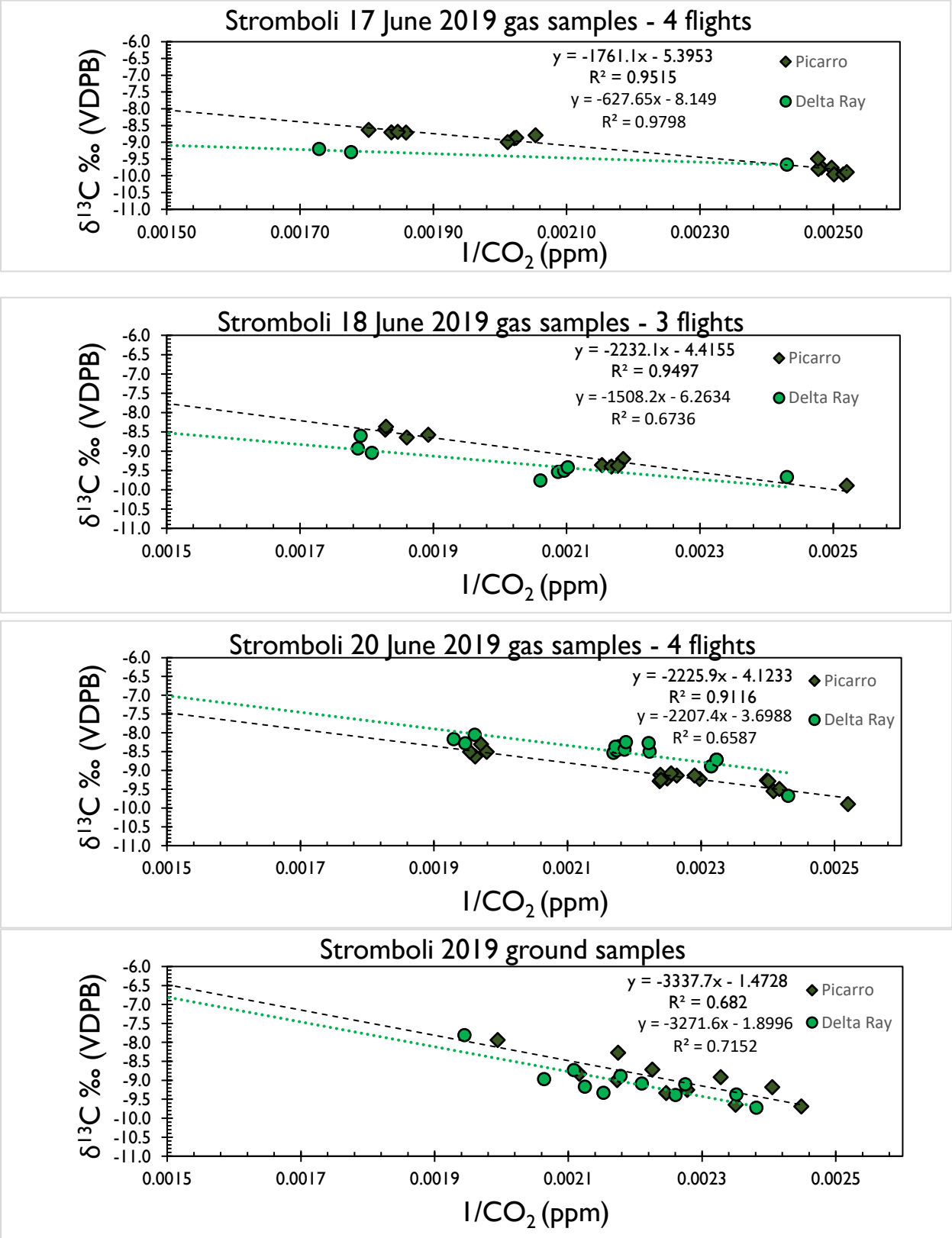

Figure S9*:* Picarro and Delta Ray data for 2019 UAS flights and ground samples.

Text S6. Comparison of Picarro and Delta Ray results for individual days in 2019

In 2019, Picarro data spans June 17, 18, and 20, while the Delta Ray data has just three datapoints from June 17 with most data from June 18 and 20. In 2019, we always flew from the pizzo and targeted the plume emanating from the central and south craters. One factor to consider here is that the plume emanations varied from one day to the next, so we plotted the individual days of data for the 2019 campaign (Figure S9). Of the four individual plots, the intercept on the 17 June is the most negative and the only plot where Delta Ray data comprises just three data points. This may explain the more negative (-8.1 ‰) intercept of the Delta Ray compared to the Picarro (-5.4‰) which has 13 data points. Interestingly, the ground samples for 2019 are much less negative than the UAS data, indicating that the ground samples may have a component of diffuse soil gas from the shallow hydrothermal system that the UAS samples directly above the plumes do not. It is notable that for all individual days of UAS flights, the data regress very well with R^2 values above 0.9 for Picarro and 0.6 for Delta Ray. It is unclear why the R^2 is so low for delta ray for the entire 2019 campaign, except that due to the large correction required to calibrate the data, the resulting values became scattered, leading to greater residuals when a linear regression was performed. Even though the combined dataset for Picarro and Delta Ray has significantly different intercepts in 2018 (-1.97 ‰) and 2019 (-5.95 %), we used the Picarro data because of the greater number of samples which were analyzed by the Picarro instrument compared to the Delta Ray. The intercomparison between the two instruments was used to examine small differences and to verify the overall consistency of our data.

Text S7. Modelling

We use a model which calculates the fraction of CO_2 remaining in the melt as a magma body rises and degasses, with starting parameters of 1000MPa, 2 wt % CO_2, NNO=0 (oxidation state). This is based on the Chosetto model of Moretti and Papale, 2004. We couple the output of this model with the closed and open degassing equations to determine the carbon isotopic signature of the melt and gas at each step of the model (Gerlach and Taylor, 1990). Heavier carbon is preferentially exsolved from a melt into the gas phase, with the gas-melt fractionation factor ranging from +2 to +4.5)(Javoy et al., 1978; Mattey, 1991). Here, we use a value of +3.5 as is common practice in recent studies (e.g., (Aubaud, 2022 and references therein). Accordingly,

$$\delta^{13}C_{gas} = \delta^{13}CO_{melt} + \Delta^{13}C_{gas-melt} \quad [5]$$

The equation for closed-system degassing we use is:

$$\delta^{13}C_{gas(residual)} = \delta^{13}CO_{melt(primordial)} - (1 - F)\Delta^{13}C_{gas-melt} \quad [6]$$

The equation for open-system degassing is:

$$\delta^{13}C_{pm} = \delta^{13}CO_{res} + 1000(1 - F^{\alpha-1}) \quad [7]$$

Data Set S1. Carbon isotopes from Stromboli volcano summit, 2018-2019

The calibrated data for the 2018 and 2019 CO_2 concentrations and carbon isotopes from Stromboli volcano

Data Set S2. Calculations of discrete carbon isotopes from Stromboli volcano summit, 2018-2019

The calibrated data and calculations using the weighted means method for the 2018 and 2019 CO_2 concentrations and carbon isotopes from Stromboli volcano. The weighted means calculations use only plume samples with volcanic CO_2 greater than 50 ppm above background as in Schipper et al. 2017